

1 **Interactions shape aquatic microbiome responses to Cu and Au nanoparticle treatments in**
2 **wetland manipulation experiments**

3

4 **Running title: Interactions mediate microbiome nanoparticle responses**

5

6 Zhao Wang¹, Christina M. Bergemann^{2,3}, Marie Simonin^{2,3,4}, Astrid Avellan^{2,5,6}, Phoebe Kiburi¹,
7 Dana E. Hunt^{1,2*}

8 ¹ Duke University Marine Laboratory, Beaufort NC USA

9 ² Center for the Environmental Implications of Nanotechnology (CEINT), Duke University,
10 Durham, North Carolina 27708, USA

11 ³ Biology Department, Duke University, Durham, North Carolina 27708, USA

12 ⁴ Present Address: University Angers, Institut Agro, INRAE, IRHS, SFR QUASAV, F-49000
13 Angers, France

14 ⁵ Department of Civil and Environmental Engineering, Carnegie Mellon University, Pittsburgh,
15 Pennsylvania 15289 USA

16 ⁶ Present Address: Géosciences Environnement Toulouse (GET), CNRS, Université de Toulouse,
17 IRD, Toulouse, France.

18

19 * Corresponding author

20

21

22

23

24

25

26 **Keywords: microbiome; nanoparticles; mesocosms; ecosystem complexity; biologically-
27 mediated interactions**

28

29 **Corresponding Author Contact Information:**

30 135 Duke Marine Lab Rd

31 Beaufort NC 28516 USA

32 dana.hunt@duke.edu

33 Phone: 252-646-9058

34 FAX: 252-504-7648

35 **Abstract**

36

37 In natural systems, organisms are embedded in complex networks where their physiology and
38 community composition is shaped by both biotic and abiotic factors. Therefore, to assess the
39 ecosystem-level effects of contaminants, we must pair complex, multi-trophic field studies with
40 more targeted hypothesis-driven approaches to explore specific actors and mechanisms. Here, we
41 examine aquatic microbiome responses to long-term additions of commercially- available
42 metallic nanoparticles [copper-based (CuNPs) or gold (AuNPs)] and/or nutrients in complex,
43 wetland mesocosms over 9 months, allowing for a full growth cycle of the aquatic plants. We
44 found that both CuNPs and AuNPs (but not nutrient) treatments showed shifts in microbial
45 communities and populations largely at the end of the experiment, as the aquatic plant
46 community senesced. we examine aquatic microbiomes under **chronic** dosing of NPs and
47 nutrients Simplified microbe-only or microbe + plant incubations revealed that direct effects of
48 AuNPs on aquatic microbiomes can be buffered by plants (regardless of seasonal As mesocosms
49 were dosed weekly, the absence of water column accumulation indicates the partitioning of both
50 metals into other environmental compartments, mainly the floc and aquatic plants
51 photosynthetically-derived organic matter. Overall, this study identifies the potential for NP
52 environmental impacts to be either suppressed by or propagated across trophic levels via the
53 presence of primary producers, highlighting the importance of organismal interactions in
54 mediating emerging contaminants' ecosystem-wide impacts.

55

56

57

58 **Funding**

59

60 This work was supported by the National Science Foundation (NSF) and the Environmental
61 Protection Agency (EPA) under NSF Cooperative Agreement EF-0830093 and DBI-1266252,
62 Center for the Environmental Implications of Nanotechnology (CEINT) and the National
63 Science Foundation (ICER: 2033934, DEB: 2224819) to DEH. Any opinions, findings,
64 conclusions or recommendations expressed in this material are those of the author(s) and do not
65 necessarily reflect the views of the NSF or the EPA. This work has not been subjected to EPA
66 review and no official endorsement should be inferred.

67

68

69

70

71

72

73

74

75

76

77

78

79

80

81 **Introduction**

82

83 Among emerging contaminants, engineered metallic nanoparticles (NPs) have received increased
84 attention as their consumer applications have expanded (Saravanan et al., 2021). NPs' small size
85 (1-100 nm) and large surface area: volume ratio generally increase their reactivity relative to
86 their bulk counterparts (Auffan et al., 2009). The biological impacts of inorganic nanoparticles
87 are generally attributed to the release of dissolution products or nano-specific effects due to their
88 physical properties. For example, metallic NPs can disrupt cell membranes and generate
89 oxidative stress, resulting in lipid and protein peroxidation and DNA damage (Clar et al., 2016;
90 Maurer-Jones et al., 2013). Concerns about NP ecotoxicity have grown, as rates of anthropogenic
91 nanoparticle deposition now rival those of natural NPs in some areas (Hochella et al., 2019).

92 While most nanomaterial studies initially focused on model NPs, there is a growing interest in
93 expanding our understanding of the ecosystem-level impacts of commercially-available NPs,
94 which primarily enter the environment through disposal or application (Carley et al., 2020;
95 Mitrano et al., 2015; Ward et al., 2019). In these commercial applications, NPs' advantages
96 include lower substrate requirements; for example, while copper has been used as a pesticide for
97 over a hundred years, newer copper-NP based biocides like Kocide® 3000 (Dupont) both
98 enhance antimicrobial properties and reduce Cu usage (Giannousi et al., 2013; Kah et al., 2018).
99 As biocides are commonly used in conjunction with other agrochemicals like fertilizers, these
100 co-occurring contaminants could alter ecosystems with impacts distinct from either the fertilizer
101 or pesticide alone (Kah, 2015).

102

103 However, it may be difficult to *a priori* predict the ecosystem outcomes of these NP-containing
104 agrochemical mixtures because of (i) NP metastability which means their (bio)transformation
105 and fate are dynamic, and differ from bulk counterparts (Avellan et al., 2020), or (ii) interactions
106 between multiple contaminants that can lead to unexpected biological impacts (Brennan and
107 Collins, 2015; Hagenbuch and Pinckney, 2012). For example, nutrients can attenuate
108 contaminant toxicity directly by binding contaminants, or indirectly by increasing the organism's
109 biomass or energy investment in detoxification (Aristi et al., 2016; Leflaive et al., 2015; Pieters
110 et al., 2005; Skei et al., 2000). Conversely, nutrients can increase toxicity through enhanced
111 contaminant uptake (Hu et al., 2013). As we cannot robustly predict ecosystem outcomes from
112 short-term, laboratory studies, recent research has focused on environmentally realistic
113 conditions including contaminant mixtures or co-occurring stressors in complex multi-trophic
114 systems.

115

116 Microbes are a critical component of all ecosystems: with high diversity, short generation times
117 and as critical mediators of biogeochemical cycles, the microbiome can be a sensitive and
118 ecologically-important indicator of disturbance (Aylagas et al., 2017; Hunt and Ward, 2015).
119 Although early NP microbiome research focused on acute exposures in bacterial model systems
120 (e.g. *Escherichia coli*), the field has shifted toward chronic exposures and whole community
121 microbiome analyses. These community-level microbiome studies incorporate key, often
122 uncultured organisms; account for different responses within microbiomes and incorporate
123 modification of NP by other organisms or ecosystem components (Chae et al., 2014; Colman et
124 al., 2014; Ward et al., 2019). Thus, there is a growing body of literature on how interactions with
125 other organisms, and their associated biomacromolecules and ligands, can alter microbial

126 responses to toxicants through competition for resources, alteration of organic matter quantity
127 and/or quality, or transformation and accumulation of contaminants (Bone et al., 2012; Ge et al.,
128 2014).

129

130 Here, to investigate how ecosystem complexity and co-occurring anthropogenic contaminants
131 shape microbial responses to NPs, we examine aquatic microbiomes under chronic dosing of
132 NPs and nutrients (N and P) in wetland mesocosms. We focus on two NPs: the commercially-
133 available agricultural biocide Kocide® 3000 [containing Cu(OH)₂ NPs] and citrate-coated gold
134 nanoparticles (AuNPs). While AuNPs were initially used primarily as a tracer of NP fate
135 (Avellan et al., 2018), they have potential commercial applications in catalysts, sensors and
136 medical treatments as well as potential ecotoxicity. Both these NP-based contaminants were
137 chronically dosed into wetland mesocosms with either nanoparticles (CuNPs or AuNPs),
138 nutrients, or both a single NP type and nutrients, over a 9-month period. Prior research on these
139 mesocosms has revealed unexpected organismal responses (Perrotta et al., 2020), NP
140 (bio)transformations (Avellan et al., 2020) and increased macroalgal blooms under chronic NP
141 and nutrient dosing (Simonin et al., 2018a). However, it is still unclear how exposure to multiple
142 stressors impacts aquatic microbial communities (Rillig et al., 2019). Further, as these
143 mesocosms contain a complex food web including fish, snails, and plants, microbiome
144 composition reflects both direct contaminant impacts and indirect effects mediated by
145 interactions with other organisms (Hunt and Ward, 2015). To directly address the issue of
146 ecosystem complexity, we employed a microcosm experiment (Bergemann et al., 2023) to
147 address AuNP treatment effects in simplified communities composed of either only microbes or
148 both microbes and the aquatic plant *Egeria densa*. Thus, this set of experiments focus on

149 identifying key environmental factors that mediate microbial responses to emerging pollutants in
150 dynamic aquatic environments.

151

152 **Methods**

153

154 **Wetland mesocosm experiments**

155 Experiments were conducted at the Center of Environmental Implications of Nanotechnology
156 (CEINT) mesocosm facility in the Duke University Forest (Durham, North Carolina, USA) from
157 January 2016 - October 2016. Details about experimental set-up and monitoring were previously
158 described (Lowry et al., 2012; Simonin et al., 2018a). Briefly, slantboard mesocosms (3.66 m
159 long, 1.22 m wide and 0.8 m high) lined with a water-tight geotextile (0.45 mm reinforced
160 polypropylene, Firestone Specialty Products, U.S.) were partially filled with sand, creating a
161 permanently flooded zone (aquatic zone), a periodically flooded zone (transition zone), and a
162 rarely flooded zone (upland zone). The mesocosms were filled with well water sourced at the site
163 with an average starting water volume of 452 L; as the water level fluctuated over time with
164 precipitation and evapotranspiration, therefore dosing is provided as weight rather than
165 concentration. Organisms were introduced sequentially prior to starting the experiment in 2015,
166 including the floating plant *Egeria densa*; aquatic snails *Physella acuta* and *Lymnaea* sp.; and the
167 fish *Gambusia holbrookii* (eastern mosquitofish). An algal and zooplankton inoculum was added
168 biweekly to reduce major divergences between mesocosms due to dispersal limitation and
169 wetland plants were seeded in the transition zone.

170

171 Mesocosms were randomly assigned to one of six treatments (three replicates per treatment):
172 control-ambient nutrient, control-nutrient enriched, AuNPs-ambient nutrient, AuNPs-nutrient
173 enriched, Kocide (CuNPs)-ambient nutrient, and Kocide (CuNPs)-nutrient enriched. The
174 synthesis and TEM characterization of citrate-stabilized AuNPs (average diameter: 11.9 ± 1.2
175 nm) and characterization of copper hydroxide NPs (average diameter: 38.7 ± 8.2 nm) (CuNPs;
176 Kocide 3000; DuPont, Wilmington, Delaware, USA) were described previously (Simonin et al.,
177 2018a). Mesocosms dosed with AuNPs received a weekly dose of 19 mg Au, resulting in a total
178 dose of 750 mg Au after 9 months. As Kocide is 27% Cu, CuNP mesocosms received an initial
179 pulse of 93.7 mg of Cu and then a weekly dose of 9.5 mg of Cu, resulting in a total dose of 450
180 mg Cu as Kocide per mesocosm after 9 months. Starting in September 2015, the nutrient-
181 enriched treatments received 1 L of mesocosm water each week supplemented with 88 mg of N
182 as KNO_3 and 35 mg of P as KH_2PO_4 to mimic agricultural run-off. This was a collaborative
183 project and the nutrient amendment conditions were part of a complex experimental design that
184 balanced the needs of many researchers, including preventing water column hypoxia.

185

186 Au and Cu concentrations in unfiltered surface water and other environmental metadata
187 including temperature were collected as previously described (Avellan et al., 2020). To examine
188 the microbial community, the aquatic zone was sampled immediately before dosing (D0), then 1
189 and 7 days (D1, D7) after dosing, as well as after the first (T1), second (T2) and third (T3)
190 quarters. At each timepoint, ~ 250 mL of water was collected from the near-surface (~ 0.25 m
191 depth) by submerging sterile polypropylene bottles, and microbial biomass was collected from
192 ~ 100 - 250 mL of water on 0.22 μm Supor filters (Pall) via gentle vacuum filtration upon return to
193 the lab. Samples were stored at -80 $^{\circ}\text{C}$ until DNA extraction.

194

195 **Jar microcosm experiments**

196

197 In this experimental follow up to the outdoor mesocosms, simplified microcosms in one-quart
198 acid-washed Ball® glass mason jars examined the impacts of ecosystem complexity and
199 seasonal conditions on AuNP-dosed microbiomes, as described previously (Bergemann et al.,
200 2023). Four treatments were chosen to compare with mesocosms mimicking both season (spring
201 and early fall) and ecosystem complexity (microbes only or microbes + *Egeria*). Environmental
202 Growth Chambers were set to match spring conditions (light: dark 12:12 hrs; irradiance 481.95
203 \pm 4.14 lum ft⁻²; temperature 15 °C and 10°C in the light and dark periods, respectively) and
204 early fall (15:9 hrs light: dark cycle; irradiance 521.65 \pm 3.08 lum ft⁻²; temperature 30 °C and 20
205 °C in the light and dark periods, respectively). We note the “season” label differs between this
206 paper and a prior publication (Bergemann et al., 2023). Both spring and fall conditions were
207 assayed for two ecosystem complexities: microbes only and microbes + *Egeria densa*, with 6
208 replicate jars for each condition. Each microcosm was filled with 100 g of washed Quickrete
209 pool filter sand 700 mL of 0.25mm filtered water collected in July 2017 from a control
210 mesocosm (described above) and 1 mL of 0.25 mm filtered local wetland water; filtration
211 removed large organisms and debris to establish a microbiome. Macrophyte-containing
212 microcosms also included five rinsed shoots of *E. densa* with a total wet weight of 6g. Weekly
213 for 5 weeks, 143.3 µg of nitrogen (N) and 56.97 µg of phosphorus (P) were added to each
214 microcosm as KNO₃ and KH₂PO₄. Each jar was capped with Parafilm® to allow the exchange of
215 gases as well as light infiltration. After a week of acclimation, the AuNPs exposures began using

216 the same AuNP stock as the mesocosm experiment with 31.36 μ g of Au added per week for a
217 total of 125.44 μ g over four weeks.

218

219 Water samples were collected to measure Au concentration and dissolved organic carbon (DOC).
220 To measure Au concentration in the microcosms, 5 mL of water was collected weekly, acidified
221 with HNO₃ and HCl, then quantified using ICP-MS (Agilent 7700 and 7900). At the end of the
222 experiment, 10 mL of GFF-filtered water was collected to measure dissolved organic carbon
223 (DOC) using a TOC-VCPh Analyzer with a TNM-1 module (Shimadzu). At the end of the
224 experiment, microbial biomass for community analysis was collected from 100 mL of water on
225 0.22 μ m Supor filters (Pall) via gentle vacuum filtration. Samples were stored at -80 °C until
226 DNA extraction.

227

228 **Nucleic acid extraction, library preparation and sequence analysis**

229

230 Genomic DNA for SSU rRNA gene libraries was extracted using the Gentra Puregene
231 Yeast/Bacteria kit (QIAGEN) supplemented with bead beating (60 seconds; Biospec), cleaned
232 using the Zymo *OneStep* PCR inhibitor removal kit and quantified using a Nanodrop ND-1000.
233 515F-926R (V4-V5) 16S rRNA gene libraries were constructed using a dual-barcode sequencing
234 approach (Needham et al., 2019; Parada et al., 2016). PCR reactions were performed in triplicate
235 with 20 μ l reactions containing 20 ng template DNA, 1 \times Taq Buffer, 0.5 μ M of each primer, 200
236 μ M of dNTPs, and 0.4 U of non-proofreading Econo Taq (Lucigen). The thermal cycling
237 conditions were 2 min at 95°C, followed by 25 cycles of 1 min at 95°C, 1 min at 50°C, 30 sec at
238 72°C, and a final extension at 72°C for 10 min. Triplicate PCR reactions were pooled and gel

239 purified (QIAquick, QIAGEN). Libraries were pooled at the same concentration, and the final
240 pooled library concentration and purity verified by TapeStation (Agilent) and sequenced at the
241 Duke Center for Genomic and Computational Biology using v2 2 x250 bp sequencing on the
242 Illumina MiSeq.

243

244 Barcodes were removed and sequences were assigned to each sample using CASAVA (Illumina)
245 and MacQIIME v1.9.1, sequences were then cleaned and clustered using USEARCH v.9.2
246 (Edgar, 2013). Low quality sequence ends were trimmed at a Phred quality score (Q) of 30 using
247 a 10 bp running window. Paired-end reads were merged if the overlap was at least 10 bp with no
248 mismatches. Sequences with expected errors >1 and/or a length <400 bp were removed. Potential
249 chimeras were filtered with *uchime2* in USEARCH v.9.2. MED v2.1 was then used to resolve
250 amplicon sequence variants (ASVs) (Eren et al., 2015), with a minimum unique sequence
251 abundance of 20. The remaining 10,374 ASVs represented 7,368,537 reads, representing 89% of
252 all reads. The taxonomies of representative ASVs were classified using MacQIIME v1.9.1 using
253 RDP classifier v2.2 (Wang et al., 2007). Mitochondrial and chloroplast sequences were removed
254 and the libraries were then sub-sampled to 8,074 reads per library. SSU rRNA library sequences
255 were deposited as Bioproject PRJNA613470.

256

257 Bray-Curtis dissimilarities were visualized using non-metric multidimensional scaling (NMDS)
258 ordination, and beta-diversity was analyzed by permutational multivariate ANOVA
259 (PERMANOVA) using the *adonis* function in the *vegan* R package (Oksanen et al., 2015). ASV
260 relative abundances >0.1%, with an added pseudo count of 1 to avoid excessive zeros inflating
261 the model, were used to identify taxa with statistically significant effects of nanoparticles

262 (CuNPs or AuNPs), nutrients or interactions between factors using DESeq2 with a multifactor
263 design (Love et al., 2014). Comparisons between environmental variables utilized the non-
264 parametric Wilcoxon signed rank test, and significant differences were identified when $p < 0.05$
265 (Benjamini-Hochberg adjusted).

266

267

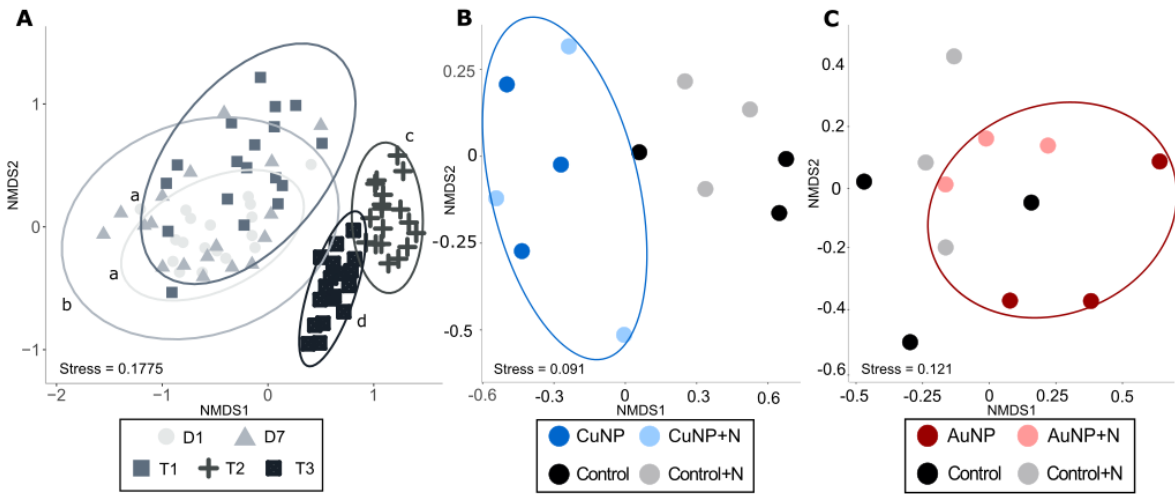
268 **Results and Discussion**

269

270 In order to characterize microbiome responses to NP-containing contaminant mixtures, here we
271 initially focus on the aquatic compartment of wetland mesocosms exposed to factorial NP and
272 nutrient treatments. In this experiment, CuNP treatments received a high initial dose (~94 mg of
273 Cu as Kocide) to mimic a high load due to storm-driven transport and then weekly doses of
274 CuNPs at concentrations approximating agricultural runoff (Simonin et al., 2018a). This
275 approach led to high initial Cu in the water column that gradually declined over time (Figure S1).

276 In contrast, AuNPs were applied at a steady rate and quickly sedimented out of the water
277 column, resulting in aquatic gold concentrations that were slightly elevated over controls
278 throughout the experiment (Figure S1). As mesocosms were dosed weekly, the absence of water
279 column accumulation indicates the partitioning of both metals into other environmental
280 compartments, mainly the floc and aquatic plants (Avellan et al., 2020). In order to understand
281 how NPs and nutrient additions might impact aquatic microbial communities, we examined
282 microbial community composition 1 day (D1) and 7 days (D7) after dosing initiation to identify
283 initial treatment effects and after 3, 6, and 9 months (T1, T2 and T3) to investigate potential
284 chronic or accumulation-driven microbiome impacts. While there were strong seasonal changes

285 in the microbial community (PERMANOVA, $p < 0.05$; Figure 1A and Table S1), we did not
286 identify a significant effect of nutrient addition alone or of NP-nutrient interactions on the
287 microbiome (Figures 1, S2, S3 and Tables S2, S3). While nutrient addition previously alleviated
288 Kocide inhibition of soil microbes (Simonin et al., 2018b), here we posit that most of the
289 heterotrophic microbes are not nutrient-limited, thus low levels of added nitrogen and
290 phosphorous did not significantly alter microbial community composition. However, prior
291 research on these mesocosms found that nutrient-amended NP treatments intensified episodic
292 macroalgal blooms, significantly altering competition between planktonic algae and floating
293 plants and other environmental parameters (Simonin et al., 2018a). Somewhat surprisingly, the
294 impact of nutrients on primary producers did not propagate to the non- eukaryotic, planktonic
295 microbiome composition examined here; but higher nutrient concentrations or an increased
296 number of mesocosm replicates might have revealed statistically-significant effects on the
297 microbiome. As nutrient additions did not significantly alter the aquatic microbiome, we focused
298 on the NP treatments by grouping the mesocosms with and without nutrient additions in
299 subsequent analyses (n=6). To identify potential nanoparticle treatment effects, we compared all
300 NP-samples versus non-NP amended controls; significant community NP treatment effects were
301 observed only in T3 for both Cu and Au NPs (Figures 1, S2, S3 and Tables S2, S3). Although the
302 CuNP treatment microbial communities separated from controls on days 1 and 7 (Figure S2),
303 samples violated the assumption of equal dispersion (betadisper, $p < 0.05$), thus expected short-
304 term CuNP treatment responses, potentially due to Cu toxicity, could not be evaluated
305 statistically (Table S2).



306

307 **Figure 1. Mesocosm microbial community compositional changes over time and in response**
308 **to Cu and Au nanoparticles (NPs) and nutrient additions (+N).** (A) Non-metric
309 multidimensional scaling (NMDS) ordination computed based on Bray-Curtis dissimilarity for
310 16S rRNA gene libraries of all samples over time. Ellipses show 95% confidence intervals
311 around the mean. Samples with different letters “a”, “b”, “c” and “d” indicate significant
312 differences over time (by combining all mesocosms at each time point regardless of treatment;
313 pairwise PERMANOVA $p<0.05$). D1 and D7 indicate days relative to the initiation of NP
314 dosing. T1 (3-month), T2 (6-month) and T3 (9-month) represent quarterly samples. Panels (B)
315 and (C) show NMDS ordination based on Bray-Curtis dissimilarity for 16S rRNA gene libraries
316 at time points where the NP-treated mesocosms (combining NP and NP+N treatments)
317 statistically differed from the non-NP amended treatments (combining Control and Control +N).
318 The ellipses in (B) and (C) were manually drawn to highlight the effect of NPs on microbial
319 community composition. (B) Shows the significant microbiome impacts CuNP-treatment in the
320 third quarter (T3; PERMANOVA, $p<0.05$). (C) Shows the significant microbiome impacts of
321 AuNP-treatment in the third quarter (T3; PERMANOVA, $p<0.05$). “+N” indicates nutrient
322 additions, which did not significantly affect microbial community composition, nor interact with
323 CuNP or AuNP at any time point (PERMANOVA, $p>0.05$).

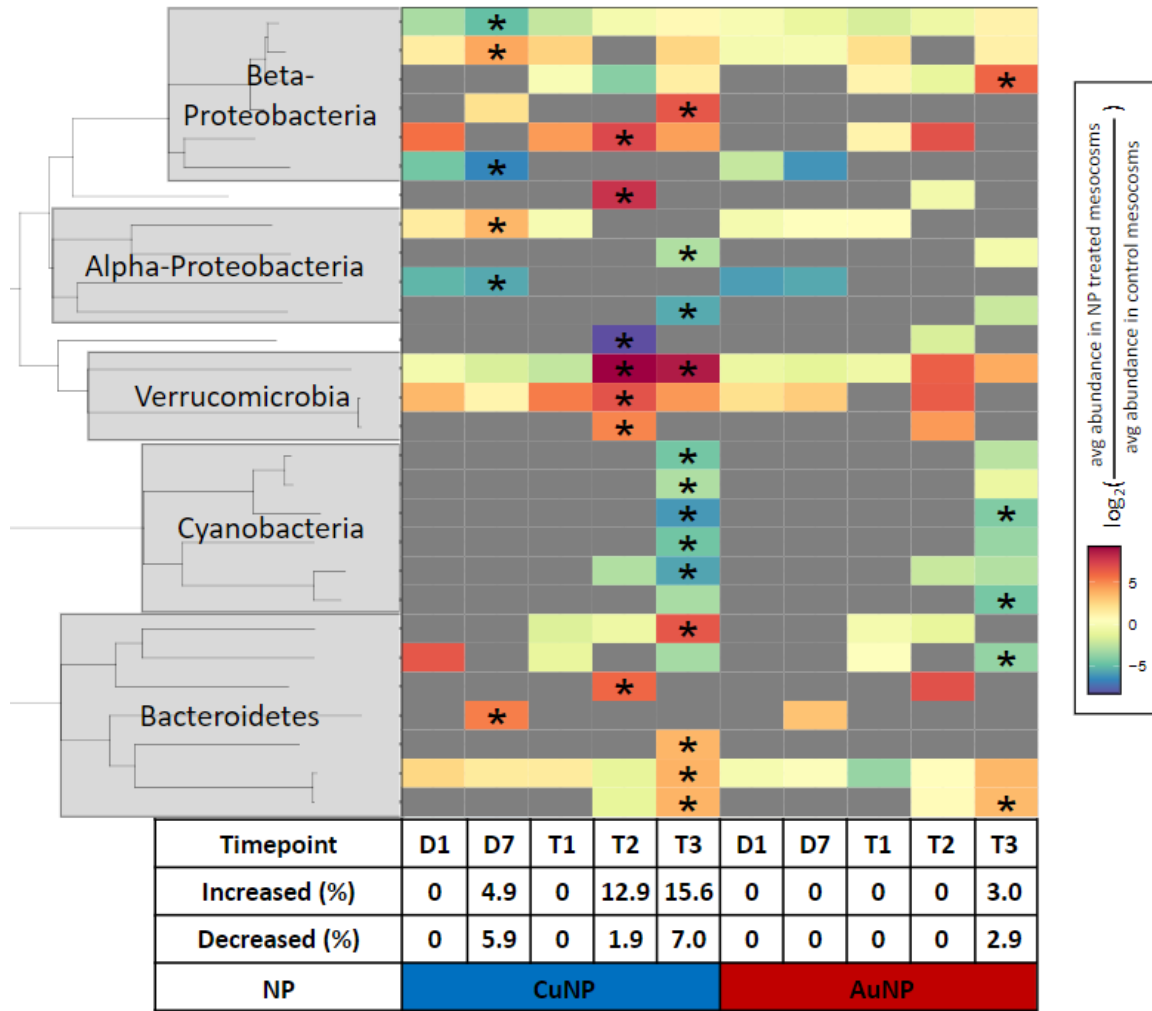
324

325 As neither metal accumulated in the aquatic compartment (Figure S1), the chronic (T3) aquatic
326 microbiome effects in both NP treatments were likely mediated by changes in the abundance or

327 physiology of other organisms (i.e. biological interactions), impacts of seasonality (e.g. effect of
328 temperature, prevalence of sensitive organisms), or changes in the speciation and bioavailability
329 of the metals (Avellan et al., 2020). Other potential explanations, such as gradual changes in the
330 microbiome due to chronic exposure, were deemed unlikely due to rapid turnover in aquatic
331 microbial populations. However, as treatments altered the balance between the macrophyte
332 *Egeria* and planktonic algae in the aquatic zone (Simonin et al., 2018a), changes in the primary
333 producer composition or metal-induced physiology could potentially alter the organic matter
334 pool available to microbial communities. We were specifically interested in explaining the
335 timing of the nanoparticle effect on microbiomes. While not a treatment effect, dissolved organic
336 carbon (DOC) declined at the end of the experiment ($\sim 5 \text{ mg L}^{-1}$ at T3 versus $>10 \text{ mg L}^{-1}$ at other
337 time points); as organic matter stabilizes and reduces the reactivity of NPs, lower organic matter
338 levels could increase the toxicity of metallic NPs or their dissolution products (Aristi et al., 2016;
339 Bone et al., 2012; Diegoli et al., 2008; Miao et al., 2009). These lower DOC levels in T3 are
340 likely due to *Egeria* senescence (Avellan et al., 2020; Simonin et al., 2018a), potentially
341 coupling ecotoxicity with plant growth stage. In addition to complexation with the nanoparticles
342 directly, labile DOC produced by actively-growing primary producers could alleviate NP-
343 toxicity by providing increased resources that allow microbial investment in detoxification etc.
344 In short, for this complex wetland experiment, we predict that the effect of NPs and their
345 transformation products on the water column microbial community are potentially predominately
346 indirect impacts mediated by complex ecosystem interactions.
347
348 In order to gain greater insight into potential NP and nutrient effects on specific taxa, we
349 examined population-level treatment responses using 16S rRNA gene amplicon sequence

350 variants (ASVs). Again, a two-factor design was applied to examine the impacts of
351 nanoparticles, nutrient additions and interactions between these two factors. For example, the
352 effect of the CuNP treatment was identified by comparing all Kocide-treated mesocosms versus
353 the mesocosms without nanoparticles, regardless of nutrient addition (n = 6). As there were not
354 significant differences between ambient and nutrient-amended treatments (Figures S4, S5), we
355 again focus on nanoparticle treatments. At the population level, CuNP treatments showed
356 significant effects on day 7 as well as at the T2 and T3 time points (Figure 2; Table S4). At the
357 beginning of the experiment (D7), taxa comprising 5.9% of the community significantly declined
358 versus 4.9% which increased in CuNP treatments compared to controls (Figure 2), suggesting a
359 balance between toxicity effects and microbes which benefit from reduced competition or
360 additional resources released by dying cells. In contrast, at later time points, a larger percentage
361 of taxa significantly increased (12.9%, 15.6%) versus declined (1.9%, 7.0 %) of the CuNP-
362 treated community in T2 and T3, respectively, suggesting that responsive phylotypes do not
363 reflect environmental toxicity but also potentially include taxa which benefit from new niches or
364 altered physiology in the NP- treatments (Figure 2). We considered a number of potential
365 explanations for the observed Cu-treatment results including copper toxicity, Cu's role as a
366 micronutrient that could stimulate growth, and ecosystem-level impacts including shifts in
367 environmental resources. Treatment-responsive taxa were spread throughout the phylogenetic
368 tree (Figure 2); however, some trends emerged which provide insight into potential mechanisms.
369 Pertaining to the toxicity hypothesis, in T3 CuNP mesocosms, several cyanobacterial ASVs
370 decreased (Table S4); these declines in cyanobacteria are consistent with either Cu toxicity or
371 changes in the balance of primary producers, as observed previously (Simonin et al., 2018a), but
372 by themselves are not conclusive. Second, we examined the potential for copper to act as a key

373 micronutrient (Clar et al., 2016; Jamers et al., 2013). As aquatic Cu concentrations are >10x
374 limiting concentrations even in non-CuNP treatments (Posacka et al., 2019), population increases
375 in CuNP-treatments are unlikely to reflect alleviation of Cu limitation. Finally, we examined the
376 evidence for ecosystem-level changes in the system; in addition to declines in cyanobacterial
377 relative abundance, in T2 CuNP treatments a number of Verrucomicrobia ASVs increased;
378 Verrucomicrobia are known polysaccharide degraders and may reflect increased environmental
379 availability of these compounds (He et al., 2017). Notably, these results contrast with previous
380 chronic AgNP treatment mesocosms (Ward et al., 2019), where similar responsive taxa were not
381 observed in both initial and long term exposure time points; the results in this study suggest
382 either strong microbiome seasonality (Figure 1) or different factors governing microbial
383 responses across the time course of the experiment. Thus, we conclude that chronic dosing of
384 CuNPs yields a complicated response, with microbial populations potentially affected by CuNP
385 treatments both directly (e.g. toxicity) and indirectly (e.g. via interactions with CuNP-responsive
386 ecosystem components), as evidenced by microbial populations that increased as well as
387 decreased in abundance. Compared to CuNP treatments, fewer taxa significantly increased or
388 decreased at any time point in AuNP treatment mesocosms (Figure 2). All 5 AuNP treatment-
389 responsive taxa were in T3; yet there was not an apparent phylogenetic signal (i.e. no clustering
390 of responsive taxa in the phylogenetic tree) and responsive taxa both increased and decreased in
391 relative abundance (Figure 2). In summary, population-level analysis shows that compared to
392 AuNPs, CuNP treatment caused more widespread impacts across both time and microbial taxa,
393 with AuNP treatment resulting in microbial community shifts relative to controls only at the end
394 of the experiment, through an unknown mechanism.



396 **Figure 2. Mesocosm amplicon sequence variants (ASVs) that significantly respond to CuNP**
 397 **or AuNP treatments.** Log₂ fold change of each ASV was calculated as
 398 $\log_2\left(\frac{\text{avg abundance in NP treated mesocosms}}{\text{avg abundance in control mesocosms}}\right)$. NP treated mesocosms include NP only and NP-
 399 nutrient enriched mesocosms (n=6), and control mesocosms include both ambient control and
 400 control + Nutrient addition mesocosms (n=6), as nutrients did not show any significant
 401 individual or interactive effect with NPs on microbial community composition. ASVs are shown
 402 in the plot if: (1) they are identified as significantly responding to CuNPs or AuNPs at any time
 403 point using DESeq2 (Asterisks indicate the taxa relative abundance was significantly different
 404 than controls $p<0.05$); and (2) ASV relative abundance exceeds the threshold of 0.2% at the
 405 corresponding time point. Gray shading indicates that the ASV does not exceed the 0.2%
 406 abundance threshold at that time point. ASVs are organized by a maximum likelihood
 407 phylogenetic tree with major phyla labelled. Underneath the heatmap, the total relative

408 abundance of ASVs that significantly increased in the NP- treated mesocosms or declined in the
409 control mesocosms are labeled with Increased (%) and Decreased (%).

410

411 **Microcosm experiments to explore ecosystem complexity in microbiome responses to NP**

412

413 The question remains why T3 (fall) samples exhibited microbiome responses in AuNP and
414 CuNP treatments, with the prediction that environmental factors rather than accumulation drives
415 this response. We specifically focus on AuNP treatments, as elemental gold was historically
416 taken as an inert tracer not toxic to microbes (Ahmad et al., 2013; Zhang et al., 2015), although
417 recent examples of microbial toxicity have been noted in the literature (Sathiyaraj et al., 2021)..

418 While the mechanisms of AuNP microbiome responses are unclear, they may include AuNP

419 antimicrobial activity of either the NPs (Sathiyaraj et al., 2021) or their environmental

420 transformation products including potentially-toxic gold ions or gold-containing compounds

421 (Avellan et al., 2018). Moreover, the fact that AuNPs mesocosms exhibited a microbiome

422 response at a single time point suggests a role for ecosystem interactions (Gräf et al., 2023),

423 which we sought to test here through guided experimentation. In addition to direct toxicity,

424 microbial community shifts could be explained by multi-stressor effects (e.g. warmer water

425 temperatures in fall samples) or indirect effects through interactions with other AuNP-treatment

426 sensitive organisms (Hunt and Ward, 2015; Wang et al., 2021). To differentiate among the

427 mechanisms behind AuNP aquatic microbiome responses and to remove co-occurring changes

428 with season (e.g. plant growth stage), we specifically tested the impact of season (spring or fall;

429 temperature and light incubations) and ecosystem complexity (presence of primary producers)

430 using simplified, month-long jar microcosms. Compared to the mesocosms, microcosms had

431 reduced organismal complexity: microbes alone or microbes incubated with the aquatic plant

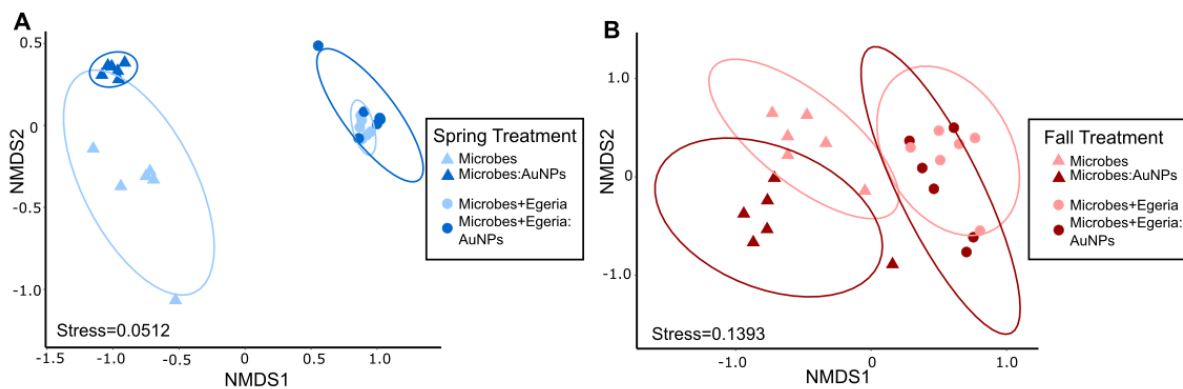
432 *Egeria*, the biomass-dominant primary producer in the aquatic compartment of the mesocosms,
433 which provides heterotrophic bacteria with carbon, competes with microbial primary producers
434 and alters water quality parameters (Figure S6). The month-long duration enables observation of
435 microbiome shifts with seasonal incubation conditions and/or AuNP treatment, without the long-
436 term accumulation effects that occurred over 9 months in the mesocosms. Microcosm conditions
437 were set to match either the beginning (spring: D1, D7) or end of the experiment (fall: T3), when
438 a significant AuNP microbiome treatment effect was observed.

439

440 In the microcosm experiment, we observed a strong season-treatment effect (Figure S7),
441 consistent with the known impact of temperature on aquatic microbial communities (Wang et al.,
442 2021; Ward et al., 2017) (Figure 3). However, contrary to our initial hypothesis of season-related
443 interactions with AuNPs, for both spring and fall regimes, AuNP treatment influenced
444 microbiome composition in the microbe-only but not in the microbiome + *Egeria* microcosms
445 (for a given ecosystem complexity and season, microbiomes were compared with or without
446 AuNP treatment: PERMANOVA, $p < 0.05$; Figure 3). Thus, the presence of *Egeria* buffers the
447 AuNP-treatment effect on microbes. Similarly, wetland plants were shown to mitigate the
448 impacts of AgNPs on microbially-mediated biogeochemical cycles (He et al., 2022) and toxicity
449 effects on juvenile fish (Bone et al., 2012), suggesting a more general role for primary producers
450 in mediating NP toxicity. Consistent with these community-level results, more AuNP treatment-
451 responsive taxa were identified in microbe-only (37) vs. microbes with *Egeria* treatments (1),
452 (Figure S8). While AuNPs were initially predicted to exhibit minimal toxicity (Zhang et al.,
453 2015), researchers have observed AuNP toxicity in microbial cultures (Ahmad et al., 2013;
454 Hernández-Sierra et al., 2008) and Au bound to ligands (e.g. cyanide, hydroxyl and thiol) has

455 unknown microbial effects (Avellan et al., 2020; Avellan et al., 2018). Responsive taxa in the
456 microcosm experiments included a number of shifts (both positive and negative) in the relative
457 abundance of Bacteroidetes, potentially reflecting replacement of AuNP-treatment-sensitive taxa
458 with resistant taxa that filled similar ecological niches (Figure S8). Thus, we examined other
459 microcosm parameters to identify potential mechanisms for *Egeria*'s mediation of AuNP's
460 microbiome impacts.

461



462

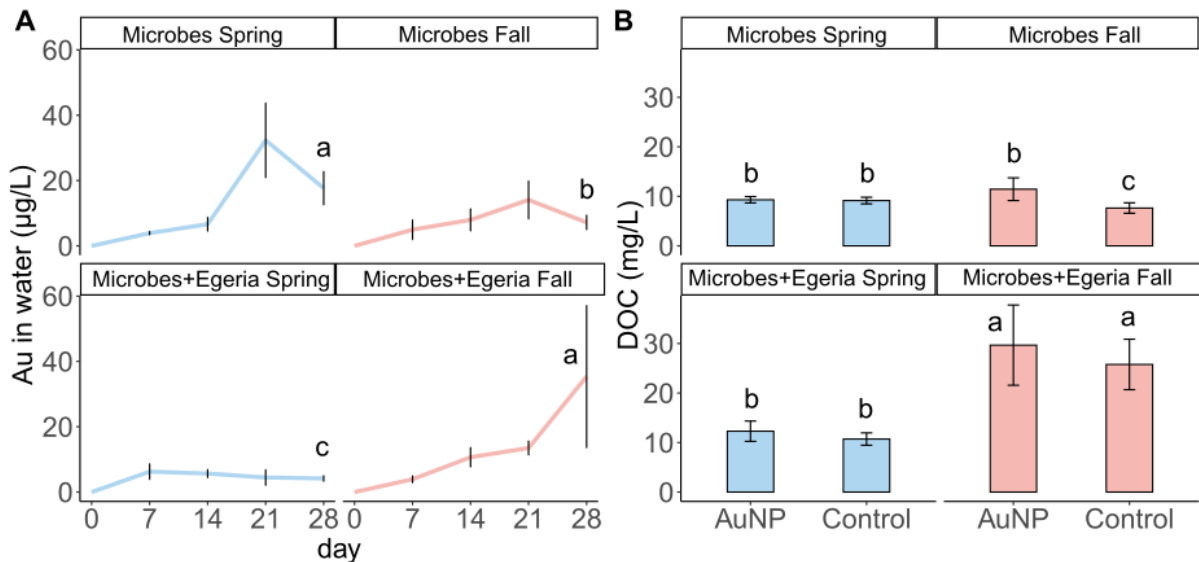
463 **Figure 3. Microcosm microbial community changes (16S rRNA gene libraries) with gold**
464 **nanoparticle conditions for different seasonal conditions and ecosystem complexity.** Jar
465 microcosm microbiomes at the end of the experiment are shown as non-metric multidimensional
466 scaling (NMDS) ordination based on Bray-Curtis dissimilarity. (A) Spring treatment conditions:
467 average 12.5 °C, light:dark: 12:12 hours (B) Fall conditions: average 26.25 °C, light:dark: 15:9
468 hours. Ellipses (95% confidence intervals around the mean) show significant effects of AuNP
469 treatment for a given seasonal treatment in the Microbe-only microcosms (PERMANOVA, $p <$
470 0.05). Triangles indicate microcosms with microbes only and circles those containing both
471 microbes and the plant *Egeria densa*.

472

473 Although AuNP treatments with *Egeria* did not exhibit shifts in microbiome composition in
474 either season, water column parameters suggest *Egeria* has different effects on the AuNPs: in

475 spring, removal of gold from the water column and in fall stabilization and inactivation of water
476 column gold through enhanced DOC concentrations (Glenn and Klaine, 2013). In the spring
477 AuNP treatment microcosms, aquatic gold concentrations are significantly higher in the microbe-
478 only condition (Figure 4A, $p < 0.05$ Wilcoxon signed- rank test), and more gold accumulated in
479 the *Egeria* (Microbe+ *Egeria* treatment) (Bergemann et al., 2023). In contrast, under fall
480 conditions, water column gold was significantly higher (mean $\sim 40 \mu\text{g L}^{-1}$) in the microbe +
481 *Egeria* AuNP treatment than in the microbe-only treatment ($\sim 10 \mu\text{g L}^{-1}$, Figure 4A, $p < 0.05$
482 Wilcoxon signed rank test). This higher aquatic gold concentrations in the fall microbe + *Egeria*
483 AuNP treatment could be explained by high *Egeria*-produced dissolved organic carbon (DOC)
484 concentrations which stabilized aquatic Au and potentially reduced its toxicity (Figure 4B;
485 $p < 0.05$ Wilcoxon signed rank test) (Aristi et al., 2016; Diegoli et al., 2008; Glenn and Klaine,
486 2013; Miao et al., 2009). As the DOC concentration is elevated in *Egeria*-containing AuNP and
487 Control treatments (Figure 4B), DOC levels are due to “fall” conditions rather than the AuNP
488 treatment. Although we cannot definitively assign a mechanism, these results complement the
489 field mesocosm’s conclusions that microbe-only studies may not readily translate to complex
490 ecosystems, where interactions with other organisms (and environmental factors) mediate
491 contaminant microbiome responses in complex and unpredicted ways. Overall, these combined
492 experiments suggest that growing aquatic plants attenuates NP-toxicity; however, this protective
493 effect is lost during *Egeria* senescence with the accompanying decline in aquatic DOC (as
494 observed in the mesocosm experiment).

495



496

497 **Figure 4. Microcosm gold and dissolved organic carbon (DOC) colonized by either**
 498 **microbes or microbes + *Egeria* incubated under spring and fall conditions.** (A) Total gold in
 499 the water column over the 28-day incubation for AuNP treatment microcosms. Means on day 28
 500 labeled with the same letter are not significantly different (Wilcoxon ranked sum test, $p < 0.05$).
 501 Error bars show one standard deviation. (B) Microcosm DOC concentrations on day 28 labeled
 502 with the same letter are not significantly different (Wilcoxon ranked sum test, $p < 0.05$). Error
 503 bars show one standard deviation. Seasonal comparisons between spring (avg. 12.5 °C,
 504 light:dark; 12:12 hours) and fall (avg. 26.25 °C, light:dark; 15:9 hours) treatments.

505

506

507 **Conclusions**

508

509 In these set of two linked experiments, we found that CuNPs and AuNPs treatments can exert
 510 significant effects on aquatic microbial communities, but that microbiome responses are likely a
 511 combination of direct effects as well as interactions with other ecosystem components. While
 512 NPs can generate broad ecosystem-level effects either as synthesized or as transformation
 513 products, as well as indirect effects mediated by interactions with other organisms (Hunt and

514 Ward, 2015), the impacts of nanoparticles are strongly mediated by environmental complexity.
515 Here, we speculate that, compared to other taxa, primary producers have the potential to either
516 suppress or propagate the effects of contaminants to other trophic levels due to their position at
517 the base of the food web and biomass dominance in many ecosystems (Ge et al., 2014;
518 Slaveykova, 2022). This research suggests that rather than requiring full-ecosystem complexity,
519 simplified microcosms containing primary producers may allow greater insights into the impacts
520 of nanoparticles and other contaminants on microbiomes. Thus, by focusing on critical
521 ecosystem components, we can better understand the processes by which contaminants transform
522 and are transformed by ecosystems.

523

524 **Acknowledgements**

525 We acknowledge contributions of the entire CEINT mesocosm team to this research, especially
526 the leadership of Emily Bernhardt.

527

528 **CRedit Statement**

529 **Zhao Wang:** Data curation, Formal analysis, Investigation, Visualization, Writing-original draft

530 **Christina M. Bergemann:** Data curation, Investigation, Writing- review and editing

531 **Marie Simonin:** Data curation, Investigation, Writing- review and editing

532 **Astrid Avellan:** Data curation, Investigation, Writing- review and editing

533 **Phoebe Kiburi:** Investigation

534 **Dana E. Hunt:** Formal analysis, Resources, Visualization, Writing-original draft

535

536

537 **References**

538

539 Ahmad, T., et al., 2013. Antifungal activity of gold nanoparticles prepared by solvothermal
540 method. *Materials Research Bulletin*. 48, 12-20.

541 Aristi, I., et al., 2016. Nutrients versus emerging contaminants—or a dynamic match between
542 subsidy and stress effects on stream biofilms. *Environmental Pollution*. 212, 208-215.

543 Auffan, M., et al., 2009. Towards a definition of inorganic nanoparticles from an environmental,
544 health and safety perspective. *Nature Nanotechnology*. 4, 634-641.

545 Avellan, A., et al., 2020. Differential Reactivity of Copper- and Gold-Based Nanomaterials
546 Controls Their Seasonal Biogeochemical Cycling and Fate in a Freshwater Wetland
547 Mesocosm. *Environmental Science & Technology*. 54, 1533-1544.

548 Avellan, A., et al., 2018. Gold nanoparticle biodissolution by a freshwater macrophyte and its
549 associated microbiome. *Nature Nanotechnology*. 13, 1072-1077.

550 Aylagas, E., et al., 2017. A bacterial community-based index to assess the ecological status of
551 estuarine and coastal environments. *Marine Pollution Bulletin*. 114, 679-688.

552 Bergemann, C. M., et al., 2023. Seasonal Differences and Grazing Pressure Alter the Fate of
553 Gold Nanoparticles in a Microcosm Experiment. *Environmental Science & Technology*.
554 57, 13970-13979.

555 Bone, A. J., et al., 2012. Biotic and abiotic interactions in aquatic microcosms determine fate
556 and toxicity of Ag nanoparticles: part 2-toxicity and Ag speciation. *Environmental
557 Science & Technology*. 46, 6925-6933.

558 Brennan, G., Collins, S., 2015. Growth responses of a green alga to multiple environmental
559 drivers. *Nature Climate Change*. 5, 892-897.

560 Carley, L. N., et al., 2020. Long-Term Effects of Copper Nanopesticides on Soil and Sediment
561 Community Diversity in Two Outdoor Mesocosm Experiments. *Environmental Science &
562 Technology*. 54, 8878-8889.

563 Chae, S.-R., et al., 2014. Aging of fullerene C₆₀ nanoparticle suspensions in the presence of
564 microbes. *Water Research*. 65, 282-289.

565 Clar, J. G., et al., 2016. Copper Nanoparticle Induced Cytotoxicity to Nitrifying Bacteria in
566 Wastewater Treatment: A Mechanistic Copper Speciation Study by X-ray Absorption
567 Spectroscopy. *Environmental Science & Technology*. 50, 9105-9113.

568 Colman, B. P., et al., 2014. Emerging Contaminant or an Old Toxin in Disguise? Silver
569 Nanoparticle Impacts on Ecosystems. *Environmental Science & Technology*. 48, 5229-
570 5236.

571 Diegoli, S., et al., 2008. Interaction between manufactured gold nanoparticles and naturally
572 occurring organic macromolecules. *Science of the Total Environment*. 402, 51-61.

573 Edgar, R. C., 2013. UPARSE: highly accurate OTU sequences from microbial amplicon reads.
574 *Nature Methods*. 10, 996-998.

575 Eren, A. M., et al., 2015. Minimum entropy decomposition: Unsupervised oligotyping for
576 sensitive partitioning of high-throughput marker gene sequences. *The ISME Journal*. 9,
577 968-979.

578 Ge, Y., et al., 2014. Soybean plants modify metal oxide nanoparticle effects on soil bacterial
579 communities. *Environmental Science & Technology*. 48, 13489-13496.

580 Giannousi, K., et al., 2013. Synthesis, characterization and evaluation of copper based
581 nanoparticles as agrochemicals against *Phytophthora infestans*. *RSC advances*. 3, 21743-
582 21752.

583 Glenn, J. B., Klaine, S. J., 2013. Abiotic and biotic factors that influence the bioavailability of gold
584 nanoparticles to aquatic macrophytes. *Environmental Science & Technology*. 47, 10223-
585 10230.

586 Gräf, T., et al., 2023. Biotic and Abiotic Interactions in Freshwater Mesocosms Determine Fate
587 and Toxicity of CuO Nanoparticles. *Environmental Science & Technology*. 57, 12376-
588 12387.

589 Hagenbuch, I. M., Pinckney, J. L., 2012. Toxic effect of the combined antibiotics ciprofloxacin,
590 lincomycin, and tylosin on two species of marine diatoms. *Water Research*. 46, 5028-
591 5036.

592 He, G., et al., 2022. Aquatic macrophytes mitigate the short-term negative effects of silver
593 nanoparticles on denitrification and greenhouse gas emissions in riparian soils.
594 *Environmental Pollution*. 293, 118611.

595 He, S., et al., 2017. Ecophysiology of freshwater Verrucomicrobia inferred from metagenome-
596 assembled genomes. *Msphere*. 2, e00277-17.

597 Hernández-Sierra, J. F., et al., 2008. The antimicrobial sensitivity of *Streptococcus mutans* to
598 nanoparticles of silver, zinc oxide, and gold. *Nanomedicine: Nanotechnology, Biology*
599 and *Medicine*. 4, 237-240.

600 Hochella, M. F., et al., 2019. Natural, incidental, and engineered nanomaterials and their
601 impacts on the Earth system. *Science*. 363, eaau8299.

602 Hu, Y., et al., 2013. Nitrate nutrition enhances nickel accumulation and toxicity in *Arabidopsis*
603 plants. *Plant and Soil*. 371, 105-115.

604 Hunt, D. E., Ward, C. S., A network-based approach to disturbance transmission through
605 microbial interactions. *Frontiers in Microbiology*, Vol. 6, 2015, pp. 1182.

606 Jamers, A., et al., 2013. Copper toxicity in the microalga *Chlamydomonas reinhardtii*: an
607 integrated approach. *Biometals*. 26, 731-740.

608 Kah, M., 2015. Nanopesticides and nanofertilizers: emerging contaminants or opportunities for
609 risk mitigation? *Frontiers in Chemistry*. 3, 64.

610 Kah, M., et al., 2018. A critical evaluation of nanopesticides and nanofertilizers against their
611 conventional analogues. *Nature Nanotechnology*. 13, 677-684.

612 Leflaive, J., et al., 2015. Community structure and nutrient level control the tolerance of
613 autotrophic biofilm to silver contamination. *Environmental Science and Pollution
614 Research*. 22, 13739-13752.

615 Love, M. I., et al., 2014. Moderated estimation of fold change and dispersion for RNA-seq data
616 with DESeq2. *Genome Biology*. 15, 1.

617 Lowry, G. V., et al., 2012. Long-term transformation and fate of manufactured Ag nanoparticles
618 in a simulated large scale freshwater emergent wetland. *Environmental Science &
619 Technology*. 46, 7027-7036.

620 Maurer-Jones, M. A., et al., 2013. Toxicity of engineered nanoparticles in the environment.
621 *Analytical Chemistry*. 85, 3036-3049.

622 Miao, A.-J., et al., 2009. The algal toxicity of silver engineered nanoparticles and detoxification
623 by exopolymeric substances. *Environmental Pollution*. 157, 3034-3041.

624 Mitrano, D. M., et al., 2015. Review of nanomaterial aging and transformations through the life
625 cycle of nano-enhanced products. *Environment International*. 77, 132-147.

626 Needham, D., et al., 2019. Fuhrman Lab 515F-926R 16S and 18S rRNA Gene Sequencing
627 Protocol V.2. protocols.io.

628 Oksanen, J., et al., 2015. Package 'vegan'. Community ecology package, version. 2.

629 Parada, A. E., et al., 2016. Every base matters: assessing small subunit rRNA primers for marine
630 microbiomes with mock communities, time series and global field samples.
631 *Environmental Microbiology*. 18, 1403-1414.

632 Perrotta, B. G., et al., 2020. Copper and Gold Nanoparticles Increase Nutrient Excretion Rates of
633 Primary Consumers. *Environmental Science & Technology*. 54, 10170-10180.

634 Pieters, B. J., et al., 2005. Influence of food limitation on the effects of fenvalerate pulse
635 exposure on the life history and population growth rate of *Daphnia magna*.
636 *Environmental Toxicology and Chemistry*. 24, 2254-2259.

637 Posacka, A. M., et al., 2019. Effects of Copper Availability on the Physiology of Marine
638 Heterotrophic Bacteria. *Frontiers in Marine Science*. 5.

639 Rillig, M. C., et al., 2019. The role of multiple global change factors in driving soil functions and
640 microbial biodiversity. *Science*. 366, 886-890.

641 Saravanan, A., et al., 2021. A review on biosynthesis of metal nanoparticles and its
642 environmental applications. *Chemosphere*. 264, 128580.

643 Sathiyaraj, S., et al., 2021. Biosynthesis, characterization, and antibacterial activity of gold
644 nanoparticles. *Journal of Infection and Public Health*. 14, 1842-1847.

645 Simonin, M., et al., 2018a. Engineered nanoparticles interact with nutrients to intensify
646 eutrophication in a wetland ecosystem experiment. *Ecological Applications*. 86, 1435-
647 1449.

648 Simonin, M., et al., 2018b. Plant and microbial responses to repeated Cu(OH)₂ nanopesticide
649 exposures under different fertilization levels in an agro-ecosystem. *Frontiers in
650 Microbiology*. 9, 1769.

651 Skei, J., et al., 2000. Eutrophication and contaminants in aquatic ecosystems. *AMBIO: A Journal
652 of the Human Environment*. 29, 184-194.

653 Slaveykova, V. I., 2022. Phytoplankton Controls on the Transformations of Metal-containing
654 Nanoparticles in an Aquatic Environment. *Environmental Nanopollutants*. 9, 113.

655 Wang, Q., et al., 2007. Naive Bayesian classifier for rapid assignment of rRNA sequences into
656 the new bacterial taxonomy. *Applied and Environmental Microbiology*. 73, 5261.

657 Wang, Z., et al., 2021. Environmental stability impacts the differential sensitivity of marine
658 microbiomes to increases in temperature and acidity. *The ISME Journal*. 15, 19-28.

659 Ward, C. S., et al., 2019. Conserved Microbial Toxicity Responses for Acute and Chronic Silver
660 Nanoparticle Treatments in Wetland Mesocosms. *Environmental Science & Technology*.
661 53, 3268-3276.

662 Ward, C. S., et al., 2017. Annual community patterns are driven by seasonal switching between
663 closely related marine bacteria. *The ISME Journal*. 11, 1412-1422.

664 Zhang, Y., et al., 2015. Antimicrobial activity of gold nanoparticles and ionic gold. *Journal of
665 Environmental Science and Health, Part C*. 33, 286-327.

